Semnan University

Journal of Heat and Mass Transfer Research

Journal homepage: https://jhmtr.semnan.ac.ir

ISSN: 2383-3068

Research Article

Effects of Diffusive Heating, Radiation Absorption and Joule Heating on MHD Mixed Convection Rotating Flow past an Inclined Porous Plates under the Influence of Hall Current and Thermal Radiation

Subhan Kanchi [a]*, Prabhakara Rao Gaddala [b], Shobalatha Gurram [a]

[a] *Department of Mathematics, Sri Krishnadevaraya University, Anantapuram-515003, Andhra Pradesh, India*

[b] *Department of Mathematics, Government Degree College (A), Anantapuram-515001, Andhra Pradesh, India*

ARTICLE INFO

Article history:

Received: 2023-11-02

Revised: 2024-05-01

Accepted: 2024-05-03

Keywords:

Diffusive heating;

Radiation absorption;

Hall current.

ABSTRACT

In this study, we examined the effects of diffusive heating, Hall current, and radiation absorption on the magnetohydrodynamic (MHD) mixed convective flow of a viscous, incompressible, electrically conducting Casson fluid along an inclined porous plate. This flow occurs in the presence of thermal radiation and chemical reactions. Using a perturbation approach, we derived solutions for the non-dimensional equations. Within the boundary layer, we analyzed how various non-dimensional factors influence the velocities, temperatures, and concentrations of the fluid. Additionally, computational analyses were conducted to explore the impact of relevant factors on the shear stress rate and the rates of heat and mass transfer. As the Hall and radiation absorption parameters increase, the velocity and temperature of the fluid also increase. Conversely, when the diffusive heating parameters increase, the fluid velocity and temperature exhibit opposite trends. Additionally, as thermal radiation increases, the temperature tends to decrease. Increasing the permeability factor reduces the skin friction coefficient, but increasing the thermal and mass Grashof numbers has the opposite effect. A higher Prandtl number leads to an increase in the Nusselt number. Lastly, the Sherwood number decreases as the amount of absorbed radiation increases.

1. Introduction

Heat and mass transfer in the context of non-Newtonian fluid flow, particularly Casson fluid flow, presents intriguing challenges and opportunities. Casson fluids exhibit non-Newtonian behavior characterized by yield stress and a nonlinear relationship between shear stress and shear rate. When studying heat and mass transfer in Casson fluid flow, several key considerations come into play. Applications of heat and mass transfer in Casson fluid flow encompass a wide range of industries, including pharmaceuticals, food processing, cosmetics, and polymer processing. Understanding the complex interplay between fluid rheology, heat transfer, and mass transfer in Casson fluid flow is essential for optimizing processes, improving efficiency, and developing innovative technologies in these fields. Swapna et al. [1] have studied Viscous Dissipation and Chemical Reactions on Radiate

* **Corresponding author.**
E-mail address: subhankanchi786@gmail.com

Cite this article as:

Kanchi, S., Gaddala, P. R., and Gurram, S., 2024. Effects of Diffusive Heating, Radiation Absorption and Joule Heating on MHD Mixed Convection Rotating Flow past an Inclined Porous Plates under the Influence of Hall Current and Thermal Radiation. *Journal of Heat and Mass Transfer Research*, 11(2), pp. 179-194.

https://doi.org/10.22075/JHMTR.2024.32228.1494

MHD Casson Nanofluid Past a Stretching Surface with a Slip Effect. Isaiah [2] has discussed the Spectral Quasi-Linearization Approach for Unsteady MHD Boundary Layer Flow of Casson Fluid Due to an Impulsively Stretching Surface. Sarojamma et al. [3] have possessed unsteady boundary layer flow of a Casson fluid past a wedge with wall slip velocity. Mustapha et al. [4] have reviewed the analysis of MHD thermosolutal convection in a porous cylindrical cavity filled with a Casson nanofluid, considering Soret and Dufour effects. Raghunath et al. [5] have discussed the effects of radiation absorption and aligned magnetic field on MHD cassion fluid past an inclined vertical porous plate in porous media. Kumar et al. [6] have possessed thermal diffusion and inclined magnetic field effects on MHD free convection flow of Casson fluid past an inclined plate in conducting field.

Magnetohydrodynamics (MHD) is a fascinating interdisciplinary field that explores the behavior of electrically conducting fluids in the presence of magnetic fields. Emerging at the intersection of fluid dynamics, electromagnetism, and plasma physics, MHD offers profound insights into a wide range of natural and engineered phenomena. From the dynamics of cosmic plasma in astrophysics to the design of advanced propulsion systems, MHD has found diverse applications across various domains. In engineering, MHD principles are utilized in numerous applications. One prominent application is magnetic confinement fusion, where MHD is crucial for controlling and stabilizing the plasma in experimental fusion reactors. MHD is also employed in the design of electromagnetic propulsion systems for spacecraft, offering a potentially efficient and environmentally friendly means of propulsion for future space missions. Moreover, MHD has applications in energy production and conversion. Srinivasacharya and Swamp Reddy [7] have analyzed Chemical reaction and radiation effects on mixed convection heat and mass transfer over a vertical plate in power-law fluid saturated porous medium. Ibrahim et al. [8] have discussed the Effect of the chemical reaction and radiation absorption on the unsteady MHD free convection flow past a semi-infinite vertical permeable moving plate with heat source and suction. Meenakshi [9] has studied the Dufour and Soret Effect on Unsteady MHD Free Convection and Mass Transfer Flow Past an Impulsively Started Vertical Porous Plate Considering Heat Generation. Aly et al. [10] have discussed Radiation and Chemical Reaction Effects on Unsteady Coupled Heat and Mass Transfer by Free Convection from a Vertical Plate Embedded in Porous Media. Narender et al. [11] have expressed Heat and mass transfer of nanofluid over a linear stretching surface with a viscous dissipation effect. Raghunath et al. [12] have discussed Radiation absorption on MHD Free Conduction flow through a porous medium over an unbounded vertical plate with a heat source.

The Dufour number denotes the contribution of the concentration gradients to the thermal energy flux in the flow. It can be seen that an increase in the Dufour number causes a rise in temperature. The interaction between radiation absorption and diffusive heating is particularly significant in scenarios where both processes coexist, such as solar collectors, atmospheric heating models, and industrial furnaces. For example, in a solar collector, sunlight is absorbed by a fluid flowing through a heat exchanger, leading to localized heating. This absorbed energy then undergoes diffusive heating as it spreads through the fluid, influencing temperature gradients and fluid flow patterns within the collector. Understanding the combined effects of radiation absorption and diffusive heating is essential for optimizing the performance of various thermal systems, improving energy efficiency, and addressing challenges related to climate change, thermal management, and materials processing. By studying the intricate interplay between these processes, researchers and engineers can develop innovative solutions to complex problems and contribute to advancements in science and technology. Khan et al. [13] have studied the Influences of Gyrotactic Microorganisms and Nonlinear Mixed Bio-convection on Hybrid Nanofluid Flow over an Inclined Extending Plate with Porous Effects. Hamma et al. [14] have discussed the Analysis of MHD Thermosolutal Convection in a Porous Cylindrical Cavity Filled with a Casson Nanofluid, Considering Soret and Dufour Effects. Mridusmita et al. [15] have analyzed the Convective MHD Flow of a Rotating Fluid Past through a Moving Isothermal Plate under Diffusion-Thermo and Radiation Absorption. Jamir and Hemanta [16] have possessed Effects of Radiation Absorption, Soret, and Dufour on Unsteady MHD Mixed Convective Flow past a Vertical Permeable Plate with Slip Condition and Viscous Dissipation. The impacts of Radiation absorption and diffusive heating have all been examined in this work [17–19].

Joule heating and thermal radiation are two significant phenomena in fluid mechanics that profoundly influence the behavior of fluids in diverse applications. Joule heating, arising from the conversion of electrical energy to heat when an electric current passes through a conductor, plays a crucial role in conductive fluid systems. In fluid mechanics, this phenomenon finds

applications in various fields, such as electrokinetic flow control, where electric fields manipulate fluid motion, and in microfluidic devices for precise temperature control and thermal actuation. Thermal radiation, on the other hand, refers to the emission of electromagnetic radiation from the surface of a body due to its temperature. In fluid mechanics, thermal radiation plays a vital role in applications involving high-temperature flows, such as combustion processes in engines and industrial furnaces. Additionally, thermal radiation is significant in radiative heat transfer, where it influences temperature distributions within fluid systems, impacting fluid flow behavior and heat transfer rates. The integration of Joule heating and thermal radiation analysis in fluid mechanics provides a comprehensive understanding of heat transfer mechanisms and facilitates the design and optimization of fluid systems for various engineering applications, ranging from microfluidics to large-scale industrial processes. Indeed, James Prescott Joule first proposed the concept of Joule heating in 1840 [20], establishing the relationship between electrical current passing through a conductor and the heat produced as a result of the electrical resistance encountered. Since then, Joule heating has garnered significant attention and has been extensively studied due to its numerous practical applications across various industries, particularly in the realm of heat transfer. In the heat transfer sector, Joule heating effects have found wide-ranging applications, including in the manufacturing of heat transfer spectacles and equipment. Loganathan and Rajan [21] have studied an entropy approach of Williamson nanofluid flow with Joule heating and zero nanoparticle mass flux. Zhou et al. [22] have studied Numerical analysis of thermal radiative Maxwell nanofluid flow over-stretching porous rotating disk. Khan et al. [23] have studied Irreversibility analysis in the hydromagnetic flow of Newtonian fluid with Joule heating: Darcy–Forchheimer model. Hafeez et al. [24] have expressed the Features of the Cattaneo–Christov double diffusion theory on the flow of non-Newtonian Oldroyd-B nanofluid with Joule heating. Shamshuddin and Eid [25] have studied nth-order reactive nano liquid through convective elongated sheets under mixed convection flow with joule heating effects. Recent research by Pramanik [26] has shown that thermal radiation and the Casson factor both increase the thermal flow rate. In their work, Khan et al. [27] examined the thermal and mass transfer properties of bioconvection nanofluid flow. They concluded after completing the research mentioned in the preceding sentence. The researchers Ahmad et al. [28] have used modeling and simulation to examine heat radiation over the same period to assess their combined effects.

The properties and behavior of porous media play a crucial role in numerous scientific and engineering fields, including hydrogeology, petroleum engineering, soil science, environmental engineering, and materials science. Understanding how fluids flow through porous media, interact with solid surfaces, and transport substances within these materials is essential for addressing a wide range of practical applications, such as groundwater management, oil recovery, pollutant transport, and filtration processes. According to the Carman-Kozeny correlation Dullien [29], the permeability increases with increasing porosity and vice versa for a fixed grain size. Moreover, the Darcy number is proportional to the permeability. Thus, the Darcy number increases with the increase in porosity and vice versa for a fixed grain size. Deepthi et al. [31] have studied the recent development of heat and mass transport in the presence of hall, ion slip, and thermo diffusion in radiative second-grade Material. Raghunath [32] has analyzed the study of heat and mass transfer of an unsteady Magnetohydrodynamic Nanofluid flow past a vertical porous plate in the presence of chemical reaction, radiation and soret effects. Raghunath et al. [33] have possessed Diffusion Thermo and Chemical Reaction Effects on Magnetohydrodynamic Jeffrey Nanofluid over an Inclined Vertical Plate in the Presence of Radiation Absorption and Constant Heat Source. Raghunath et al. [34] have looked at Heat and mass transfer on the MHD flow of Jeffrey nanofluid based on Cu and TiO2 over an inclined plate and diffusion-thermo and radiation absorption effects.

Hall Effect is a fundamental principle in fluid mechanics that describes the behavior of charged particles, such as ions or electrons, in a conductive fluid (plasma or electrolyte) under the influence of an applied magnetic field and an electric current. Named after physicist Edwin Hall, who discovered it in 1879, the Hall Effect manifests itself as a transverse electric field perpendicular to both the direction of the current flow and the magnetic field. In fluid mechanics, the Hall effect is particularly significant in plasma physics, where charged particles are abundant. When a magnetic field is applied perpendicular to the direction of ion flow within a plasma, it exerts a force on the charged particles, causing them to experience a Lorentz force. This force deflects the charged particles perpendicular to both the magnetic field and the direction of the current flow, resulting in the accumulation of charge on opposite sides of the plasma, creating an electric field. This electric field, in turn, modifies the

plasma's behavior and fluid dynamics. Sunitha et al. [35] Unsteady MHD rotating mixed convective flow through an infinite vertical plate subject to Joule heating, thermal radiation, Hall current, and radiation absorption. Hari Babu et al. [36] have possessed Heat and Mass Transfer on Unsteady MHD Chemically Reacting Rotating Flow of Jeffrey Fluid Past and Inclined Plates under the Impact of Hall Current, Diffusion Thermo, and Radiation Absorption. Raghunath et al. [37] have expressed Investigation of MHD Casson fluid flow past a vertical porous plate under the influence of thermal diffusion and chemical reaction. Raghunath et al. [38] have reviewed the Hall current and thermal radiation effects of 3D rotating hybrid Nanofluid reactive flow via stretched plate with internal heat absorption. Raghunath et al. [39] have studied the unsteady magneto-hydro-dynamics flow of Jeffrey fluid through porous media with thermal radiation, Hall current, and Soret effects.

The novelty of this work lies in the investigation of magnetohydrodynamic (MHD) mixed convective flow of a Casson fluid along an inclined porous plate. The study integrates diffusive heating, Hall current effects, radiation absorption, and chemical reactions within the framework of the flow analysis. The inclusion of these multiple influencing factors, offering insights into the interplay between various physical phenomena. Furthermore, the use of a perturbation approach to derive solutions for the non-dimensional equations demonstrates a rigorous mathematical treatment of the problem. Additionally, the analysis extends beyond theoretical derivations to include computational analyses, providing a holistic understanding of the flow behavior and its implications on shear stress rates and heat and mass transfer rates. Overall, the study contributes to advancing the understanding of MHD flows involving non-Newtonian fluids and porous media under the influence of various physical effects, thereby offering valuable insights for both theoretical and practical applications.

2. Non-Newtonian Fluid Model

The rheological equation of state for an isotropic incompressible flow of a Casson fluid [40] can be expressed as:

$$\tau_{ij} = \begin{cases} 2\left(\mu_B + \dfrac{P_y}{\sqrt{2\pi}}\right) e_{ij}, \pi > \pi_{c,} \\ 2\left(\mu_B + \dfrac{P_y}{\sqrt{2\pi_C}}\right) e_{ij}, \pi < \pi_{c,} \end{cases} \quad (1)$$

in equation (1), $\pi = e_{ij}, e_{ij}$, Where e_{ij} are the $(i, j)th$ Component of the deformation rate, π is the product of the deformation rate with itself, π_C is a critical value of this product based on the non-Newtonian model, μ_B is the plastic dynamic viscosity of the non-Newtonian fluid and P_y the yield stress of the fluid.

3. Formulation of the Problem

In a rotating system, we investigated the mixed convective flow of a viscous non-squishing fluid with the effects of hall currents and Joule heating. The fluid transfers electricity via an inclined porous plate submerged in a uniform porous media. We examined diffusion, thermodynamic absorption, and radiation absorption. The electrically conducting fluid spins as it moves over the plate. We have discussed this subject in great detail, and it has been on our minds. The z-axis is perpendicular to the plate, and the x-axis descends on it; this is the Cartesian coordinate system we looked at (see Figure 1). The fluid and the plate rotate as a rigid body with a uniform angular velocity Ω about z-axis in the presence of an imposed uniform magnetic field B_0 normal to the plate. The induced magnetic field is tiny compared to external magnetic field. All the physical variables are independent of x, as the motion is two dimensional and length of the plate is large. A homogenous first order chemical reaction between fluid and the species concentration is taken into account in which the rate of chemical reaction is directly proportional to the species concentration.

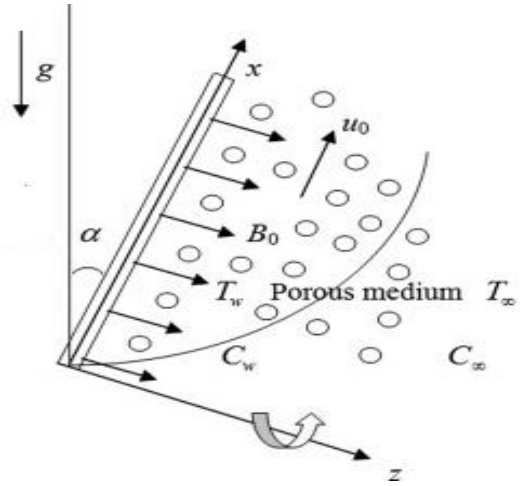

Fig. 1. Physical phenomena of the Problem

This should be done while keeping in mind the assumptions made earlier in this section by [31].

$$\frac{\partial w}{\partial z} = 0 \Rightarrow w = -w_0 \left(w_0 > 0\right) \quad (2)$$

$$w\frac{\partial u}{\partial z}+2\Omega w=\vartheta\left(1+\frac{1}{\lambda}\right)\frac{\partial^2 u}{\partial z^2}+\frac{J_x B_0}{\rho}-\frac{\vartheta}{k}u+ g\left[\beta_T(T-T_\infty)+\beta_C(C-C_\infty)\right]Cos\alpha \quad (3)$$

$$w\frac{\partial w}{\partial z}-2\Omega u=\vartheta\left(1+\frac{1}{\lambda}\right)\frac{\partial^2 w}{\partial z^2}-\frac{J_y B_0}{\rho}-\frac{\vartheta}{k}w \quad (4)$$

$$w\frac{\partial T}{\partial z}=\frac{k_1}{\rho C_p}\frac{\partial^2 T}{\partial z^2}+\frac{\vartheta}{C_p}\left[\left(\frac{\partial u}{\partial z}\right)^2+\left(\frac{\partial w}{\partial z}\right)^2\right]+\frac{\sigma B_0^2}{\rho C_p}\left(u^2+w^2\right)+\frac{Q_0}{\rho C_p}(T-T_\infty)-\frac{1}{\rho C_p}\frac{\partial q_r}{\partial z}+Q_1\left(C-C_\infty\right)+\frac{DK_T}{C_s C_p}\frac{\partial^2 C}{\partial z^2} \quad (5)$$

$$w\frac{\partial C}{\partial z}=D\frac{\partial^2 C}{\partial z^2}-K_c(C-C_\infty) \quad (6)$$

In the case that the assumptions described earlier turn out to be accurate, the following will serve to establish the appropriate boundary conditions for the distributions of velocity, temperature, and concentration

$$u\to 0,\quad w\to 0,\quad T\to T_\infty,\ C\to C_\infty \quad \text{as} \quad z\to\infty \quad (7)$$

$$u=0,\quad w=0,\ T=T_w,\ C=C_w \text{ at } z=0 \quad (8)$$

If Hall currents are considered, the generalised version of Ohm's law, which is followed by [30], may be written using the following form.

$$\bar{J}=\frac{\sigma}{\left(1+m^2\right)}\left(\bar{E}+\bar{V}\times\bar{B}-\frac{1}{\sigma n_e}\bar{J}\times\bar{B}\right) \quad (9)$$

In addition to this, we are operating under the assumption that the electric field E=0 gradually decreases to

$$J_x-mJ_y=-\sigma B_0 w \quad (10)$$

$$J_y+mJ_x=\sigma B_0 u \quad (11)$$

After working out the previous equations (10) and (11), we get

$$J_x=(mu-w)\frac{\sigma B_0}{1+m^2} \quad (12)$$

$$J_y=(mw+u)\frac{\sigma B_0}{1+m^2} \quad (13)$$

The resulting equations are substituting the equations (12) and (13) in (3) and (4) respectively

$$w\frac{\partial u}{\partial z}+2\Omega w=\vartheta\left(1+\frac{1}{\lambda}\right)\frac{\partial^2 u}{\partial z^2}+\frac{\sigma B_0^2}{\rho\left(1+m^2\right)}\left(mw-u\right)-\frac{v}{k}u+g\left[\beta_T(T-T_\infty)+g\beta_C(C-C_\infty)\right]\text{Cos}\alpha \quad (14)$$

$$w\frac{\partial w}{\partial z}-2\Omega u=\vartheta\left(1+\frac{1}{\lambda}\right)\frac{\partial^2 w}{\partial z^2}-\frac{\sigma B_0^2}{\rho\left(1+m^2\right)}\left(mu-w\right)-\frac{\vartheta}{k}w \quad (15)$$

By combining equations (2) and (3), we get the following result: let q = u+iw.

$$w\frac{\partial q}{\partial z}+2i\Omega q=v\left(1+\frac{1}{\lambda}\right)\frac{\partial^2 q}{\partial z^2}-\frac{\sigma B_0^2}{\rho}\frac{q}{\left(1+im\right)}-\frac{\vartheta}{k}q+g\left[\beta_T(T-T_\infty)+\beta_C(C-C_\infty)\right]\text{Cos}\alpha \quad (16)$$

There is also self-absorption for an optically thick fluid in addition to discharge, and typically the absorption quantity is dependent upon a wavelength and high enough that can consider the Roseland approximation for the radiative heat flux q_r is specified by

$$q_r=\frac{-4\sigma_1}{3k_1}\frac{\partial T^4}{\partial z} \quad (17)$$

where k_1 and σ_1 are the coefficient of mean absorption & Stefan Boltzmann constant, respectively. The temperature deviation within the flow is presumed to be adequately insignificant such that T'^4 can be represented as a linear temperature function that is achieved by elaborating over T_∞' in Taylor's series and ignoring the terms of the higher-order, thereby

$$T^4\approx 4T_\infty^3 T-3T_\infty^4 \quad (18)$$

After that, Equations (17) and (18) are included into Equation (5), which results in

$$w\frac{\partial T}{\partial z}=\frac{k_1}{\rho C_p}\frac{\partial^2 T}{\partial z^2}+\frac{\vartheta}{C_p}\left[\left(\frac{\partial u}{\partial z}\right)^2+\left(\frac{\partial w}{\partial z}\right)^2\right]+\frac{\sigma B_0^2}{\rho C_p}\left(u^2+w^2\right)+\frac{16\sigma_1 T_\infty^3}{\rho C_p 3k_1}\frac{\partial^2 T}{\partial z^2}+\frac{Q_0}{\rho C_p}(T-T_\infty)+Q_1\left(C-C_\infty\right)+\frac{DK_T}{C_s C_p}\frac{\partial^2 C}{\partial z^2} \quad (19)$$

The following are dimensionless variables that will be introduced.

$$q^*=\frac{q}{w_0},w^*=\frac{w}{w_0},\ z^*=\frac{w_0 z}{\vartheta},\theta=\frac{T-T_\infty}{T_w-T_\infty},\phi=\frac{C-C_\infty}{C_w-C_\infty},$$

$$M^2=\frac{\sigma B_0^2\vartheta}{\rho w_0^2},\text{Pr}=\frac{\vartheta\rho C_p}{k_1}=\frac{v}{\alpha},R_d=\frac{kk_1}{4\sigma_1 T_\infty'^3},\lambda_1=1+\frac{1}{\lambda},$$

$$Gr=\frac{vg\beta(T_w-T_\infty)}{w_0^3}, Gm=\frac{\vartheta g\beta^*(C_w-C_\infty)}{w_0^3},$$
$$E_c=\frac{w_0^2}{C_p(T_w-T_\infty)}, R=\frac{\Omega\vartheta}{w_0^2}, Sc=\frac{\vartheta}{D}, K=\frac{w_0^2k}{\vartheta^2},$$
$$Q=\frac{\vartheta Q_0}{\rho C_p w_0^2},\ K_r=\frac{\vartheta K_c}{w_0^2}, Q_1=\frac{\vartheta Q_1(C_w-C_\infty)}{w^2{}_0(T_w-T_\infty)}. \quad (20)$$

When non-dimensional variables are used, the set of governing equations, which includes (2) through (5), simplifies to

$$\lambda_1\frac{\partial^2 q}{\partial z^2}+\frac{\partial q}{\partial z}-\left(\frac{M^2}{1+im}+2iR+\frac{1}{K}\right)q= -Gr\,\theta Cos\alpha-Gm\,\phi Cos\alpha \quad (21)$$

$$\frac{\partial^2\theta}{\partial z^2}+\Pr\frac{\partial\theta}{\partial z}+Ec\Pr\left(\frac{\partial q}{\partial z}\right)^2+Ec\Pr M^2q^2 = \Pr(Q-Rd)\theta+Q_1\varphi D_u\frac{\partial^2\varphi}{\partial z^2} \quad (22)$$

$$\frac{\partial^2\phi}{\partial z^2}+Sc\frac{\partial\phi}{\partial z}-ScK_c\phi=0 \quad (23)$$

The equations that connect to the perimeter requirements are as shadows:

$$q=0,\ \theta=1,\quad \phi=1 \quad \text{at } z=0$$
$$q\to 0,\ \theta\to 0,\ \phi\to 0 \quad \text{as} \quad z\to\infty \quad (24)$$

4. Solution Methodology

The set of Equations (21) – (23) are partial differential equations which cannot be solved in closed form. However, these can be solved by reducing them into a set of ordinary differential equations using the following perturbation method. We now represent the velocity, temperature and concentration distributions in terms of harmonic and non-harmonic functions as

$$q=q_0(z)+E_c\,q_1(z)+O(Ec^2),$$
$$\theta=\theta_0(z)+E_c\,\theta_1(z)+O(Ec^2), \quad (25)$$
$$\phi=\phi_0(z)+E_c\,\phi_1(z)+O(Ec^2),$$

Substituting Equations (25) into Equations (21)–(23), and equating the harmonic and non-harmonic terms, and neglecting the higher order terms of ε, we obtain the following pairs of equations of order zero and order one.

$$\lambda_1 q_0''+q_0'-\left[\frac{M^2}{1+im}+2iR+\frac{1}{K}\right]q_0= (-Gr\,\theta_0-Gm\,\phi_0)Cos\alpha \quad (26)$$

$$\lambda_1 q_1''+q_1'-\left[\frac{M^2}{1+im}+2iR+\frac{1}{K}\right]q_1 = \begin{pmatrix}-Gr\,\theta_1-Gm\,\varphi\end{pmatrix}\mathrm{Cos}\alpha \quad (27)$$

$$\theta_0''+\Pr\theta_0'+\Pr(Q-Rd)\theta_0 = -\Pr(Q_1\phi_0+D_u\,\phi_0'') \quad (28)$$

$$\theta_1''+\Pr\theta_1'+\Pr(Q-Rd)\theta_1 = -\Pr\left((q_0')^2+Q_1\,\phi_1+M^2q_0+D_u\,\phi''\right) \quad (29)$$

$$\varphi_0''+Sc\varphi_0'-Sc\,Kc\,\varphi_0=0 \quad (30)$$

$$\phi_1''+Sc\phi_1'-(n+K_c)Sc\phi_1=0 \quad (31)$$

The prerequisites that connect to each perimeter are as shadows:

$$q_0=0,\ \theta_0=1,\ \phi_0=1, q_1=0,\ \theta_1=1,\ \phi_1=1 \text{ at } z=0$$
$$q_0\to 0,\theta_0\to 0,\phi_0\to 0, q_1\to 0,\theta_1\to 0,\phi_1\to 0 \text{ as } z\to\infty \quad (32)$$

Following is a list of solutions that may be achieved by applying boundary conditions (32) and translating equations (26) through (31).

$$q_0=b_3\exp(-m_1z)+b_4\exp(-m_3z)+b_5\exp(-m_4z) \quad (33)$$

$$\begin{aligned}q_1=&\,b_{16}\exp(-m_6z)+b_{16}\exp(-m_5z)+b_{17}\exp(-2m_4z)\\&+b_{18}\exp(-2m_1z)+b_{19}\exp(-2m_3z)\\&+b_{20}\exp\left(-(m_1+m_4)\right)z+b_{21}\exp\left(-(m_1+m_3)\right)z\\&+b_{22}\exp\left(-(m_3+m_4)\right)z+b_{23}\exp(-m_4)z\\&+b_{24}\exp(-m_1)z+b_{25}\exp(-m_3)z+b_{26}\exp(-m_6)z\end{aligned} \quad (34)$$

$$\theta_0=b_1\exp(-m_1z)+b_2\exp(-m_3z) \quad (35)$$

$$\begin{aligned}\theta_1=&\,b_6\exp(-2m_4z)+b_7\exp(-2m_1z)+b_8\exp(-2m_3z)\\&+b_9\exp\left(-(m_1+m_4)\right)z+b_{10}\exp\left(-(m_1+m_3)\right)z\\&+b_{11}\exp\left(-(m_3+m_4)\right)z+b_{12}\exp(-m_4)z+b_{13}\exp(-m_1)z\\&+b_{14}\exp(-m_3)z+b_{15}\exp(-m_5)z\end{aligned} \quad (36)$$

$$\phi_0=\exp(-m_1z) \quad (37)$$

$$\phi_1=0 \quad (38)$$

Putting in new values for equations (33)–(38) by solving equation (25), we can determine the field's velocity, temperature, concentration and physical quantities.

$$q = b_3\exp(-m_1 z) + b_4\exp(-m_3 z) + b_5\exp(-m_4 z) + E_c\begin{bmatrix}(b_{16}\exp(-m_6 z) + b_{16}\exp(-m_5 z) + b_{17}\exp(-2m_4 z) + \\ b_{18}\exp(-2m_1 z) + b_{19}\exp(-2m_3 z) + b_{20}\exp\left(-(m_1+m_4)\right)z + \\ b_{21}\exp\left(-(m_1+m_3)\right)z + b_{22}\exp\left(-(m_3+m_4)\right)z + b_{23}\exp(-m_4 z) + \\ b_{24}\exp(-m_1 z) + b_{25}\exp(-m_3 z) + b_{26}\exp(-m_6 z)\end{bmatrix} \quad (39)$$

$$\theta = b_1\exp(-m_1 z) + b_2\exp(-m_3 z) + E_c\begin{bmatrix}(b_6\exp(-2m_4 z) + b_7\exp(-2m_1 z) + b_8\exp(-2m_3 z) + \\ b_9\exp\left(-(m_1+m_4)\right)z + b_{10}\exp\left(-(m_1+m_3)\right)z + b_{11}\exp\left(-(m_3+m_4)\right)z + \\ b_{12}\exp(-m_4 z) + b_{13}\exp(-m_1 z) + b_{14}\exp(-m_3 z) + b_{15}\exp(-m_5 z)\end{bmatrix} \quad (40)$$

$$\phi = \exp(-m_1 z) \quad (41)$$

$$\tau = \left(\frac{\partial q}{\partial z}\right)_{z=0} = -\left(\begin{matrix}b_3 m_1 + b_4 m_3 + b_5 m_4 + \\ E_c\begin{bmatrix}b_{16}m_6 z + b_{16}m_5 + 2b_{17}m_4 + 2b_{18}m_1 + 2b_{19}m_3 + \\ b_{20}(m_1+m_4) + b_{21}(m_1+m_3) + b_{22}(m_3+m_4) + \\ b_{23}m_4 + b_{24}m_1 + b_{25}m_3 + b_{26}m_6\end{bmatrix}\end{matrix}\right) \quad (42)$$

$$Nu = -\left(\frac{\partial\theta}{\partial z}\right)_{z=0} = b_1 m_1 + b_2 m_3 + E_c\begin{bmatrix}(2b_6 m_4 + 2b_7 m_1 + 2b_8 m_3 + b_9(m_1+m_4) + \\ b_{10}(m_1+m_3) + b_{11}(m_3+m_4) + b_{12}m_4 + \\ b_{13}m_1 + b_{14}m_3 + b_{15}m_5\end{bmatrix} \quad (43)$$

$$Sh = -\left(\frac{\partial\phi}{\partial z}\right)_{z=0} = m_1 z \quad (44)$$

5. Validation for the Present Investigation

Table 4 demonstrates that the present primary velocity results, influenced by parameters such as thermal and mass Grashof numbers, permeability of porous media, and magnetic field parameters, closely align with the previously reported findings by Deepthi et al. [31]. This suggests a strong agreement between our current study and the prior research conducted by Deepthi et al. [31].

6. Results and Discussion

The effects of the governing flow parameters on the velocity, temperature and concentration distributions have been presented in Figures (2-12), respectively. Further, the effects of the flow parameters on the skin friction, Nusselt number, and rate of mass transfer have been discussed with the help of Tables (1-3). Some fixed values of the parameters are considered such as Prandtl number Pr = 0.71, which represents air at 200℃, Schmidt number Sc = 0.22 (for Hydrogen) and 0.6 (for water vapor), thermal Grashof number Gr = 5, solutal Grashof number Gm = 5, Chemical reaction (Kr) = 1, hall parameter (m)=0.5, Hartmann number (M) = 1, heat source parameter (Qo)= 0.2, radiation absorption parameter (Q_1)=1.0, angle of inclination(α)=π/3, Casson parameter (λ)=1.5, rotation parameter (Ω) = 0.2, thermal radiation parameter (R)= 1 , Dufour number Du = 1.5.

Figs. 2-3 depict the influence of thermal and concentration buoyancy forces on the primary and secondary fluid velocities. Gr represents the relative strength of thermal buoyancy force to viscous force and Gm represents the relative strength of concentration buoyancy force to viscous force. Therefore, Gr decreases on increasing the strengths of thermal buoyancy force whereas Gm increases on increasing the strength of concentration buoyancy force. In this problem natural convection flow induced due to thermal and concentration buoyancy forces; therefore, thermal buoyancy force tends to retard the primary and secondary fluid velocities whereas concentration buoyancy force tends to accelerate primary and secondary fluid velocities throughout the boundary layer region which is clearly evident from figs. 2-3. It is revealed from fig. 2 that the primary fluid velocity u increases on increasing Gr in a region near to the surface of the plate and it decreases on increasing Gr in the region away from the plate, secondary fluid velocity w decreases on increasing Gr throughout the boundary layer region. The same behavior was observed with increased Gm.

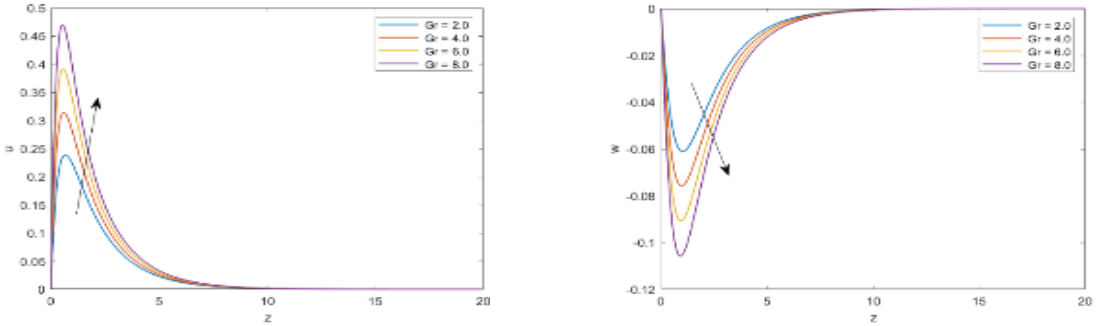

Fig. 2. The Primary and secondary velocity for *u* and *w* against *Gr*

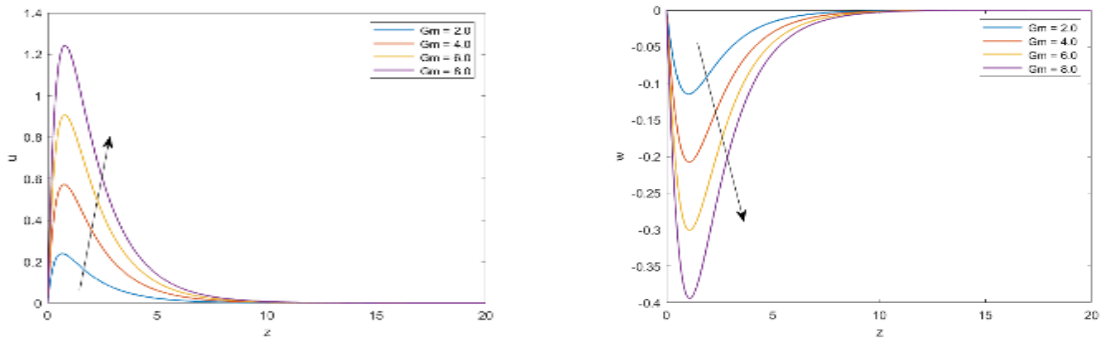

Fig. 3. The Primary and secondary velocity for *u* and *w* against *Gm*

Fig 4 shows the effect of angle of inclination, the resultant velocity diminishes with rising values of the angle of inclination.

From the figure 5, we observed that the primary diminishes and secondary velocity enhances when the intensity of the magnetic field *M* is increased. It's because the introduction of a transverse magnetic field produces a resistive type force (Lorentz force) that acts like a drag force, resisting fluid flow and lowering its velocity. In addition, when the Hartmann number raises, the thickness of the boundary layer decreases.

As seen in Figure 6, higher Casson fluid parameter values tend to slow down the fluid flow in terms of the generated final velocity. Forecasts indicate that an increase will be used to reduce yield stress. More plastic dynamic viscosity will arise, impeding liquid flow and other fluids. Additionally, plastic dynamic viscosity will increase in value. Since this highlights the fluid's flexibility, it is significant to observe that the Casson fluid's non-Newtonian behaviours become less noticeable when applied. The juice then behaves just as a Newtonian fluid would. This is a crucial topic that needs to be discussed.

Figure 7 demonstrates the effect of Hall current on the primary velocity u and secondary velocity w respectively. It is perceived from Figure. 7 that the primary velocity u enhances on increasing m throughout the boundary layer region whereas secondary velocity w diminishes on increasing m throughout the boundary layer region. This implies that, Hall current tends to accelerate primary fluid velocity throughout the boundary layer region which is consistent with the fact that Hall current induces primary flow in the flow-field whereas it has a reverse effect on secondary fluid velocity throughout the boundary layer region.

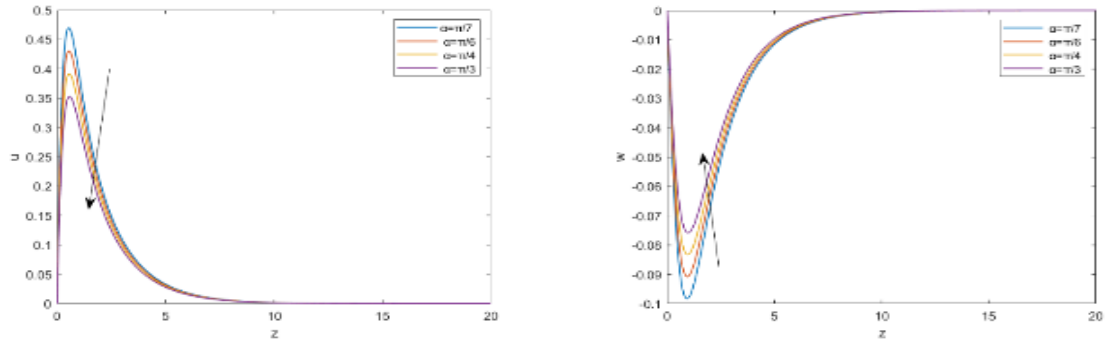

Fig. 4. The Primary and secondary velocity for *u* and *w* against *α*

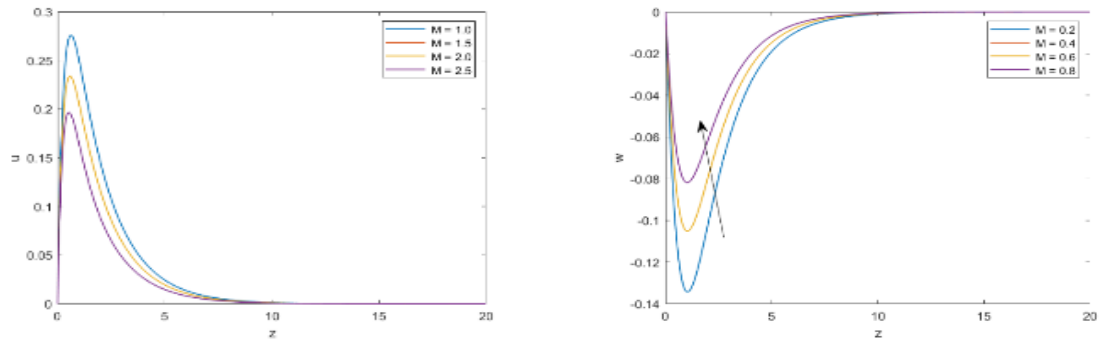

Fig. 5. The Primary and secondary velocity for *u* and*w* against *M*

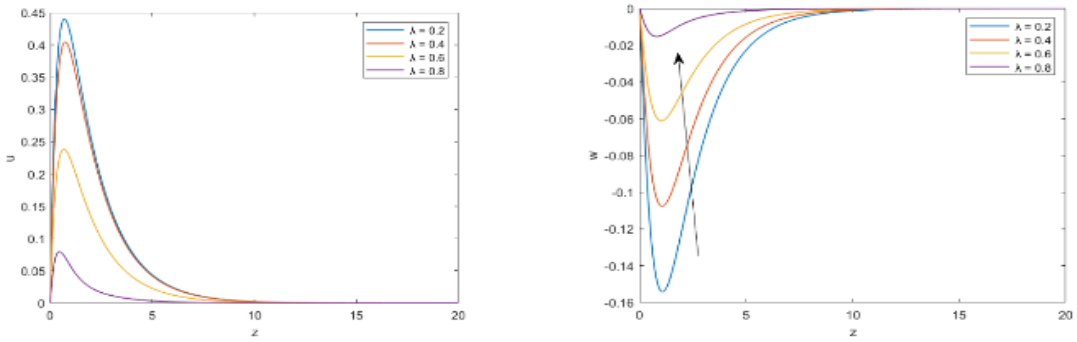

Fig. 6. The Primary and secondary velocity for *u* and *w* against λ

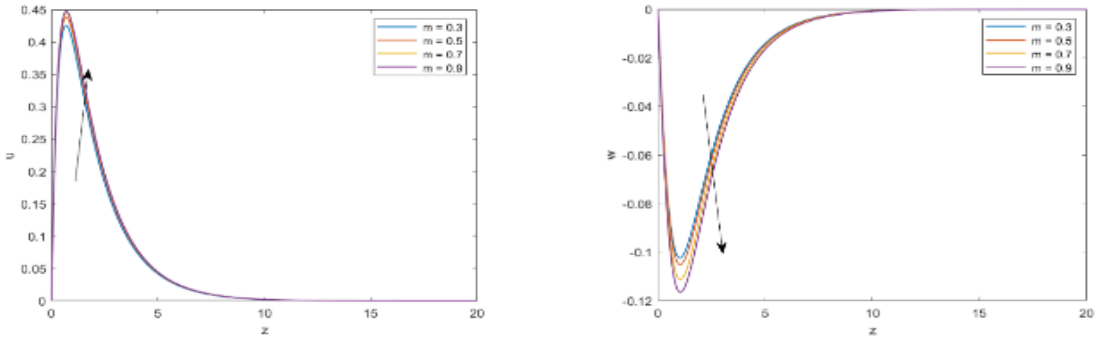

Fig. 7. The Primary and secondary velocity for *u* and *w* against *m*

Figures 8 and 10 show the effect of the radiation absorption parameter on velocity and temperature respectively. It is clear from these graphs that both velocity and temperature raises as the radiation absorption parameter rises. Because thermal radiation is linked with high temperature. The opposite behavior has been observed in secondary velocity.

In Figures 9 and 11, the impact of diffusion heating on velocity and temperature, respectively, is depicted. The decrease in primary velocity and enhancement in secondary velocity signify the alteration in fluid flow patterns due to the influence of diffusion heating. Physically, diffusion heating leads to the redistribution of thermal energy within the fluid, causing changes in the velocity field. The increase in temperature with rising values of diffusion heating indicates the absorption of heat energy by the fluid, resulting in elevated temperatures throughout the flow domain. This phenomenon can be attributed to the conversion of electrical energy to heat energy in the presence of electrical conductivity, characteristic of magnetohydrodynamic (MHD) flows. Overall, the observed trends highlight the intricate coupling between thermal and flow dynamics in the presence of diffusion heating, underscoring its significance in understanding and analyzing complex fluid system.

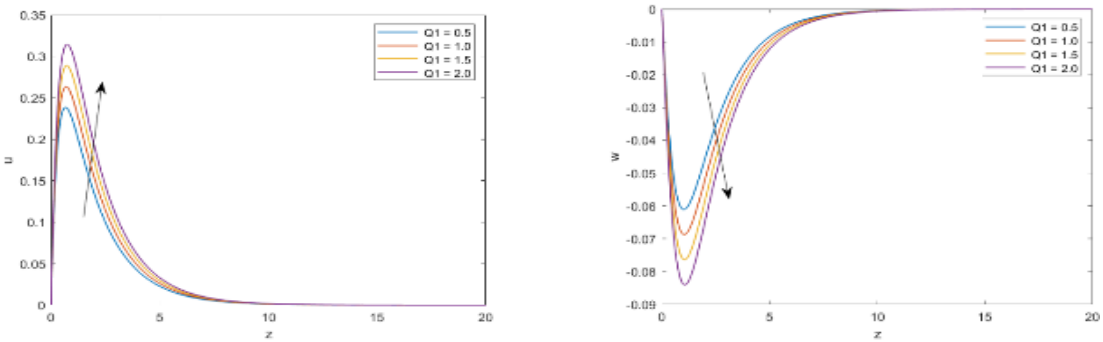

Fig. 8. The Primary and secondary velocity for *u* and *w* against Q_1

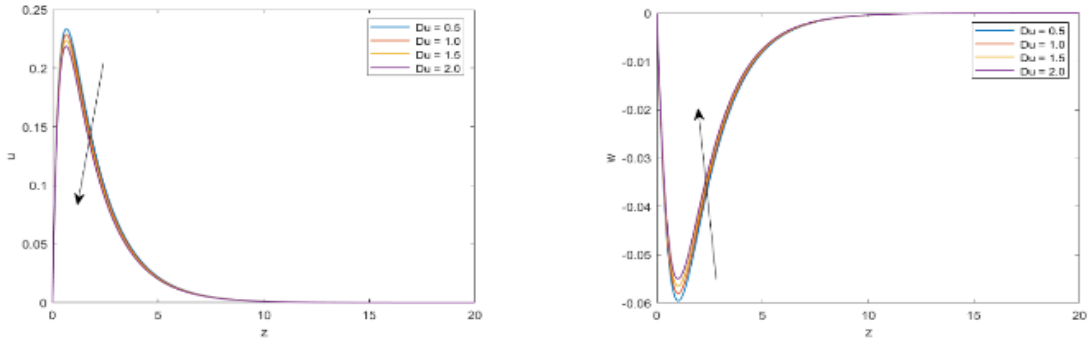

Fig. 9. The Primary and secondary velocity for u and w against D_u

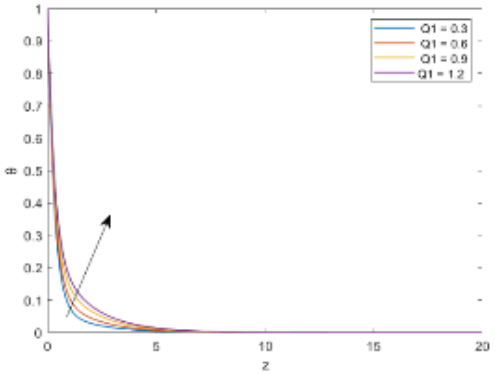

Fig. 10. The Temperature for θ against Q_1

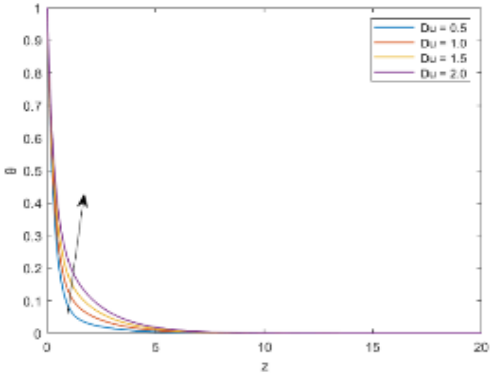

Fig. 11. The Temperature for θ against Du

In Fig. 12, the observed reduction in the concentration profile as the chemical reaction parameter (Kr) increases indicates the significant influence of chemical reactions on mass transport. As Kr enhances, chemical reactions become more dominant, leading to a decrease in the concentration buoyancy effects within the fluid. Consequently, the concentration diminishes as a consequence of intensified reactions, reflecting the consumption or production of species involved in the chemical reaction. Moving to Fig. 13, the impact of the Schmidt number (Sc) on concentration distribution is elucidated. The Schmidt number represents the ratio of momentum diffusivity to mass diffusivity and characterizes the diffusive transport of mass in the fluid. As Sc increases, indicating a decrease in mass diffusivity relative to momentum diffusivity, the ability of the fluid to transport mass diminishes. This results in a reduction in the concentration of the fluid, as mass diffuses more slowly relative to momentum, leading to a broader and less concentrated mass distribution. These findings underscore the intricate interplay between chemical reactions and mass transport, as well as the dependence of mass diffusion on fluid properties, both of which are critical factors in understanding and optimizing complex fluid system.

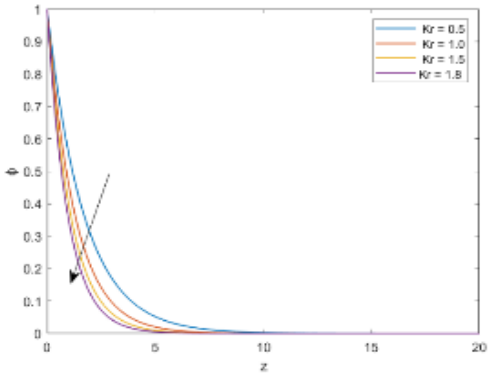

Fig. 12. The Concentration for ϕ against Kr

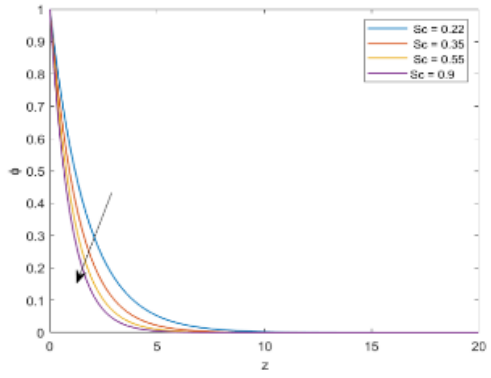

Fig. 13. The Concentration for ϕ against Sc

The data presented in Table 1 elucidates the influence of multiple parameters on skin friction in fluid flow, revealing distinct trends that underscore the intricate relationship between various physical factors and the rate of shear stress. Specifically, an increase in parameters

such as permeability of porous media (k), Hall parameter (m), thermal Grashof number (Gr), mass Grashof number (Gm), radiation absorption (Q1), and diffusive heating (Du) correlates with heightened skin friction, indicating greater fluid resistance attributed to factors like intensified electromagnetic forces, enhanced buoyancy-driven motion, and increased heat generation. Conversely, skin friction decreases with rising values of magnetic field parameter (M), angle of inclination (α), Casson fluid parameter (λ), and thermal radiation parameter (Rd), reflecting reduced fluid resistance owing to diminished magnetic field influence, altered fluid rheology, and decreased thermal radiation absorption. These findings offer crucial insights for understanding and optimizing fluid flow behavior across a broad spectrum of engineering and scientific applications.

Table 1. Skin friction (Pr=0.71; Q_0=0.2; Sc=0.22; Ec=0.01).

M	**K**	**m**	**Gr**	**Gm**	**Kr**	**Q_1**	**Rd**	**λ**	**Du**	τ
1.0	0.5	0.5	5	5	1.0	0.5	0.5	1.5	1.5	1.3155
0.6	0.5	0.5	5	5	1.0	0.5	0.5	1.5	1.5	1.2695
0.8	0.5	0.5	5	5	1.0	0.5	0.5	1.5	1.5	1.2436
1.0	0.6	0.5	5	5	1.0	0.5	0.5	1.5	1.5	1.5187
1.0	0.8	0.5	5	5	1.0	0.5	0.5	1.5	1.5	1.6747
1.0	0.5	1.0	5	5	1.0	0.5	0.5	1.5	1.5	1.4102
1.0	0.5	1.5	5	5	1.0	0.5	0.5	1.5	1.5	1.5002
1.0	0.5	0.5	5	5	1.0	0.5	0.5	1.5	1.5	1.5896
1.0	0.5	0.5	5	5	1.0	0.5	0.5	1.5	1.5	1.4636
1.0	0.5	0.5	6	5	1.0	0.5	0.5	1.5	1.5	1.5306
1.0	0.5	0.5	8	5	1.0	0.5	0.5	1.5	1.5	1.5927
1.0	0.5	0.5	5	2	1.0	0.5	0.5	1.5	1.5	1.5761
1.0	0.5	0.5	5	4	1.0	0.5	0.5	1.5	1.5	1.6194
1.0	0.5	0.5	5	5	1.5	0.5	0.5	1.5	1.5	1.5638
1.0	0.5	0.5	5	5	1.8	0.5	0.5	1.5	1.5	1.4191
1.0	0.5	0.5	5	5	1.0	0.6	0.5	1.5	1.5	1.4928
1.0	0.5	0.5	5	5	1.0	0.9	0.5	1.5	1.5	1.4165
1.0	0.5	0.5	5	5	1.0	0.5	0.6	1.5	1.5	1.5194
1.0	0.5	0.5	5	5	1.0	0.5	0.9	1.5	1.5	1.4526
1.0	0.5	0.5	5	5	1.0	0.5	0.5	2.0	1.5	1.4995
1.0	0.5	0.5	5	5	1.0	0.5	0.5	2.5	1.5	1.4137
1.0	0.5	0.5	5	5	1.0	0.5	0.5	1.5	0.3	1.5646
1.0	0.5	0.5	5	5	1.0	0.5	0.5	1.5	0.6	1.5903

According to the data presented in Table 2, the significance of the Nusselt number (Nu) increases with rising values of the Prandtl number (Pr), indicating a stronger correlation between momentum and thermal diffusivities. Additionally, Nu increases with higher levels of heat absorption (Q0) and the diffusive heating parameter (Du), suggesting enhanced convective heat transfer and diffusion-driven heat generation within the fluid. However, this trend undergoes a shift when greater amounts of thermal radiation (Rd), the Hartmann number (M), and radiation absorption (Q1) are considered. The increase in thermal radiation (Rd) may introduce complexities in heat transfer mechanisms, altering the balance between radiation and convection. Similarly, higher values of the Hartmann number (M) and radiation absorption (Q1) indicate stronger magnetic field effects and greater absorption of radiation, respectively, potentially modifying the fluid flow and heat transfer characteristics. Consequently, the significance of Nu may either stabilize or diminish with these factors, depending on the specific interactions between radiation, magnetic field, and convective heat transfer processes.

Table 2. Nusselt number (Gr=5; Gm=5; Sc=0.22; Du=0.5, Ec=0.01; Kr=1).

Pr	M	Q_0	Rd	Q_1	Du	Nu
0.71	1.0	0.2	0.5	0.5	0.5	1.6356
2	1.0	0.2	0.5	0.5	0.5	1.6936
3	1.0	0.2	0.5	0.5	0.5	1.7696
0.71	0.6	0.2	0.5	0.5	0.5	1.6937
0.71	0.8	0.2	0.5	0.5	0.5	1.6195
0.71	1.0	0.3	0.5	0.5	0.5	1.5336
0.71	1.0	0.6	0.5	0.5	0.5	1.6286
0.71	1.0	0.2	1.0	0.5	0.5	1.6495
0.71	1.0	0.2	1.5	0.5	0.5	1.6127
0.71	1.0	0.2	0.5	1.0	0.5	1.6195
0.71	1.0	0.2	0.5	1.5	0.5	1.5526
0.71	1.0	0.2	0.5	0.5	1.0	1.5795
0.71	1.0	0.2	0.5	0.5	1.5	1.6286

Table 3 illustrates the varying trends of the Sherwood number (Sh) with respect to different influencing factors. It is observed that Sh increases with the Schmidt number (Sc), thermal radiation (Rd), and the chemical reaction factor (Kr), indicating enhanced convective mass transfer and greater mass transport efficiency. Conversely, Sh decreases with rising radiation absorption (Q1) and the diffusive heating parameter (Du), suggesting a reduction in mass transfer rates possibly due to alterations in fluid flow dynamics and temperature distributions. These findings underscore the intricate interplay between various parameters influencing mass transfer phenomena, crucial for optimizing mass transfer processes and designing efficient fluid systems in diverse engineering and scientific applications.

Table 3. Sherwood number. (Gr=3; Gm=1; m=1; Q_1=0.5; Rd=0.5; Pr=0.71; Q_0=0.1; Sc=0.22; Ec=0.01)

Sc	Rd	Kr	Q_1	Du	Sh
0.22	1.0	1.0	1.0	0.5	1.4896
1	1.0	1.0	1.0	1.0	1.5496
2	1.0	1.0	1.0	1.0	1.5836
0.22	1	1.0	1.0	1.0	1.5686
0.22	1.5	1.0	1.0	1.0	1.6176
0.22	1.0	1.3	1.0	1.0	1.5275
0.22	1.0	1.6	1.0	1.0	1.5886
0.22	1.0	1.0	1.0	1.0	1.6386
0.22	1.0	1.0	1.5	1.0	1.5374
0.22	1.0	1.0	1.0	1.0	1.5646
0.22	1.0	1.0	1.0	1.5	1.4523

Table 4. Comparison of results for primary velocity (Kc = Q1 = α=Du=λ=Rd = 0).

M	K	Gr	Gm	Deepthi et al. [31]	Present Values
	0.5	5	5	0.75209	0.75273
6	0.5	5	5	0.45236	0.45287
8	0.5	5	5	0.302874	0.30025
1.0	0.6	5	5	0.78536	0.78857
1.0	0.8	5	5	0.84287	0.84947

7. Conclusion

In the present study, we thoroughly investigated the impact of radiation absorption and diffusive heating on an MHD free convective flow of a rotating Casson fluid in the presence of chemical reaction and heat source. Our comprehensive analysis yielded several crucial findings, which we outline as follows.

- An increase in radiation absorption has been found to progressively enhance fluid velocity in our study. Conversely, we observed an opposite trend with the diffusive heating parameter.

- We found that the temperature increases with higher values of both the radiation absorption and diffusive heating parameters.
- The resultant velocity decreases with increasing values of the Casson fluid parameter, angle of inclination, and magnetic field parameters. Conversely, we noted opposite behavior in the case of thermal and mass Grashof numbers.
- The fluid velocity decreases as the magnetic parameter increases. A rise in the casson parameter also results in a reduction in velocity.
- Hall current has a contrasting impact on the preliminary liquid velocity than on the secondary liquid velocity across the frontier coating area.
- We found that the concentration decreases as the Schmidt number and chemical reaction parameters increase.

Nomenclature

x^*, y^*	Coordinate system
u, w	Velocity in x and z directions (m/s)
T	Dimensional temperature of the fluid (K)
T_∞	Temperature far away from the plate (K)
T_w	Temperature near the plate (K)
C	Dimensional concentration fluid (Kgm^{-3})
C_w	Concentration near the plate (Kgm^{-3})
C_∞	Concentration from the plate (Kgm^{-3})
g	Acceleration due to gravity (ms^{-2})
k	Permeability of porous medium (m^2)
B_0	Applied magnetic field (A/m)
C_p	Fluid heat at constant pressure (JKg^{-1})
B	Magnetic field vector (A/m)
B_0	Applied magnetic field (A/m)
q_r	Heat flux (W/m^2)
E	Electric field (c)
V	Velocity vector (m/s)
J	Current density vector (A/m^2)
G_r	Thermal Grashof number
G_m	Mass Grashof number
Pr	Prandtl number
R	Rotation parameter
S_c	Schmidt number
E_c	Eckert number
M	Magnetic parameter
Q_1	Radiation absorption parameter
Du	Non dimensional Dufour number
Kr	Chemical reaction parameter
τ	Skin friction coefficient
Nu	Nusselt number
Sh	Sherwood number

Greek Symbols

ω_e	Cyclotron frequency (e/mB)
λ	Casson parameter
Du	Non dimensional Dufour number
τ_e	Electron collision time (s)
σ	Electrical conductivity (sm^{-1})
ώ	Angular velocity (r/s)
ν	Kinematic viscosity of the fluid ($m2\ s^{-1}$)
ρ	Fluid density (Kgm^{-3})
ϕ	Non-dimensional concentration fluid
θ	Non-dimensional temperature of the fluid
β	Coefficient of thermal expansion (K^{-1})
β^*	Coefficient of mass expansion ($m3\ Kg^{-1}$)

Superscripts

*	Dimensional parameters

Funding Statement

This research did not receive any specific grant from funding agencies in the public, commercial, or not-for-profit sectors.

Conflicts of Interest

The author declares that there is no conflict of interest regarding the publication of this article.

References

[1] Swapna, D., Govardhan, K., Narender, G. and Misra, S., 2023. Viscous Dissipation and Chemical Reaction on Radiate MHD Casson Nanofluid Past a Stretching Surface with a Slip Effect. Journal of Heat and Mass Transfer Research, 10, 2, 315-328. doi: 10.22075/jhmtr.2024.31758.1477.

[2] Isaiah, A.F., 2022. Spectral Quasi-Linearization Approach for Unsteady MHD Boundary Layer Flow of Casson Fluid Due to an Impulsively Stretching Surface. Journal of Heat and Mass Transfer Research, 9, 2, 269-278. doi: 10.22075/jhmtr.2016.422.

[3] Sarojamma, G., Sreelakshmi, K., Vasundhara, B., 2017. Unsteady boundary layer flow of a Casson fluid past a wedge with wall slip velocity. Journal of Heat and Mass Transfer Research, 4, 2, 91-102. doi: 10.22075/jhmtr.2017.1647.1110

[4] Mustapha El hamma, Ilham, A., Taibi, M., Rtibi, A., Kamal, G., 2023. Analysis of MHD Thermosolutal Convection in a Porous Cylindrical Cavity Filled with a Casson Nanofluid, Considering Soret and Dufour Effects. Journal of Heat and Mass Transfer Research, 10, 2, 197-206. doi: 10.22075/jhmtr.2023.30532.1439.

[5] Raghunath, K., Ramachandra Reddy, V., Obulesu, M., 2021. Effects of Radiation Absorption and Aligned Magnetic Field on MHD Cassion Fluid Past an Inclined Vertical Porous Plate in Porous Media. Published in Simulation and Analysis of Mathematical Methods in Real-Time Engineering Applications, 273–291.

[6] Pavan Kumar, C., Raghunath, K., Obulesu, M., 2021. Thermal Diffusion And Inclined Magnetic Field Effects On MHD Free Convection Flow of Casson Fluid Past an Inclined Plate In Conducting Field. Turkish Journal of Computer and Mathematics Education, Vol.12 No.13, 960-977.

[7] Srinivasacharya, D., and Swamp Reddy, G., 2016. Chemical reaction and radiation effects on mixed convection heat and mass transfer over a vertical plate in power-law fluid saturated porous medium. Journal of the Egyptian Mathematical Society, 24, 108-115.

[8] Ibrahim, F.S., Elaiw, A.M., Bakr, A.A., 2008. Effect of the chemical reaction and radiation absorption on the unsteady MHD free convection flow past a semi-infinite vertical permeable moving plate with heat source and suction. Commun. Nonlinear Sci. Numer. Simul. 13, 1056–1066.

[9] Meenakshi. V., 2021. Dufour and Soret Effect on Unsteady MHD Free Convection and Mass Transfer Flow Past an Impulsively Started Vertical Porous Plate Considering with Heat Generation. Journal of Heat and Mass Transfer Research, 8, 2, 257-266. doi: 10.22075/jhmtr.2021.21229.1301

[10] Aly, A., Chamkha, A.J., Raizah, Z.A.S., 2020. Radiation and Chemical Reaction Effects on Unsteady Coupled Heat and Mass Transfer by Free Convection from a Vertical Plate Embedded in Porous Media. Journal of Heat and Mass Transfer Research, 7, 2, 95-103. doi: 10.22075/jhmtr.2019.10763.1149

[11] Narender, G., Sreedhar Sarma, G., Govardhan, K., 2019. Heat and mass transfer of nanofluid over a linear stretching surface with viscous dissipation effect. Journal of Heat and Mass Transfer Research, 6, 2, 117-124. doi: 10.22075/jhmtr.2019.15419.1214

[12] Raghunath, K., Obulesu. M., Venkateswara Raju, K., 2023. Radiation absorption on MHD Free Conduction flow through porous medium over an unbounded vertical plate with heat source. International Journal of Ambient Energy, Volume 44(1), Pages 1712-1720. DOI:10.1080/01430750.2023.2181869

[13] Khan, A., Jawad, M., Ali, I., 2024. Influences of Gyrotactic Microorganisms and Nonlinear Mixed Bio-convection on Hybrid Nanofluid Flow over an Inclined Extending Plate with Porous Effects. Journal of Heat and Mass Transfer Research, doi: 10.22075/jhmtr.2024.32014.1485

[14] El hamma, M., Ilham, A., Taibi, M., Rtibi, A., Gueraoui, K., 2023. Analysis of MHD Thermosolutal Convection in a Porous Cylindrical Cavity Filled with a Casson Nanofluid, Considering Soret and Dufour Effects. Journal of Heat and Mass Transfer Research, 10, 2, 197-206. doi: 10.22075/jhmtr.2023.30532.1439

[15] Mridusmita, B., Nazibuddin, A., 2023. Convective MHD Flow of a Rotating Fluid Past through a Moving Isothermal Plate under Diffusion-Thermo and Radiation Absorption. Journal of Heat and Mass Transfer Research, 10, 2, 245-256. doi: 10.22075/jhmtr.2023.31013.1454

[16] Jamir, T., Hemanta, K., 2022. onwar. Effects of Radiation Absorption, Soret and Dufour on Unsteady MHD Mixed Convective Flow past a Vertical Permeable Plate with Slip Condition and Viscous Dissipation. Journal of Heat and Mass Transfer Research, 9, 2, 155-168. doi: 10.22075/jhmtr.2023.28693.1399

[17] Omar, T.B., Raghunath, K., Ali, F., Khalid, M., El Sayed Mohamed Tag-ElDin, Oreijah, M., Guedri, K., Khedher, N.B., Ijaz Khan, M., 2022. Hall Current and Soret Effects on Unsteady MHD Rotating Flow of Second-Grade Fluid through Porous Media under the Influences of Thermal Radiation and Chemical Reactions. Catalysts, 12, 1233. https://doi.org/10.3390/catal12101233.

[18] Aruna, G., Haribabu, K., Venkaeshwarlu, K., Raghunath, K., 2022. An unsteady MHD flow of a second-grade fluid passing through a porous medium in the presence of radiation absorption exhibits Hall and ion slip effects. Heat Transfer, Volume 51, 1-27. doi:10.1002/htj.2271.

[19] Raghunath, K., Mohanaramana, R., 2022. Hall, Soret, and rotational effects on unsteady MHD rotating flow of a second-grade fluid through a porous medium in the presence of chemical reaction and aligned magnetic field. International Communications in Heat and Mass Transfer, Volume 137, 106287. https://doi.org/10.1016/j.icheatmasstransfer.2022.106287.

[20] Joule, J.P., 1843, December. On the production of heat by voltaic electricity. In Abstracts of the Papers Printed in the Philosophical Transactions of the Royal Society of London (No. 4, pp. 280-282). London: The Royal Society.

[21] Loganathan, K., Rajan, S., 2020. An entropy approach of Williamson nanofuid fow with Joule heating and zero nanoparticle mass fux. J. Term. Anal. Calorim. 141, 2599–2612, 33.

[22] Zhou, S.S., Bilal, M., Khan, M. A. Muhammad, T., 2021. Numerical analysis of thermal radiative Maxwell nanofuid fow over-stretching porous rotating disk. Micromachines 12, 540.

[23] Khan, S. A. et al., 2022. Irreversibility analysis in hydromagnetic fow of Newtonian fuid with Joule heating: Darcy–Forchheimer model. J. Pet. Sci. Eng. 212, 110206.

[24] Hafeez, A., Khan, M., Ahmed, A., Ahmed, J., 2022. Features of Cattaneo–Christov double difusion theory on the fow of non-Newtonian Oldroyd-B nanofuid with Joule heating. Appl. Nanosci. 12, 265–272.

[25] Shamshuddin, M.D., Eid, M.R., 2022. nth order reactive nanoliquid through convective elongated sheet under mixed convection fow with joule heating efects. J. Term. Anal. Calorim. 147, 3853–3867.

[26] Pramanik, S., 2014. Casson fuid fow and heat transfer past an exponentially porous stretching surface in presence of thermal radiation. Ain Shams Eng. J. 5, 205–212.

[27] Khan, M. I., Shah, F., Khan, S. U., Ghafari, A., Chu, Y., 2022. Heat and mass transfer analysis for bioconvective fow of Eyring Powell nanofuid over a Riga surface with nonlinear thermal features. Numer. Methods Partial Difer. Equ. 38, 777–793.

[28] Ahmad, S., Ashraf, M., Ali, K., 2021. Simulation of thermal radiation in a micropolar fuid fow through a porous medium between channel walls. Journal Term. Anal. Calorim. 144, 941–953.

[29] Dullien, F.A.L., 1992. Porous media – fluid transport and pore structure, 2nd Edition. Academic Press, San Diego.

[30] Cowling, G.S., 1957. Magneto hydrodynamics. Interscience Publishers, New York.

[31] Deepthi, V. V. L., Maha M.A.L, Ravi Kumar, N., Raghunath, K., Ali, F., Oreijah, M., Kamel, G., El Sayed Mohamed Tag-ElDin, Ijaz Khan, M., Ahmed M. Galal., 2022. Recent Development of Heat and Mass Transport in the Presence of Hall, Ion Slip and Thermo Diffusion in Radiative Second Grade Material: Application of Micromachines. Micromachines, 13, 10: 1566. https://doi.org/10.3390/mi13101566.

[32] Raghunath, K., 2023. Study of Heat and Mass Transfer of an Unsteady Magnetohydrodynamic Nanofluid Flow Past a Vertical Porous Plate in the Presence of Chemical Reaction, Radiation and Soret Effects. Journal Of Nanofluids, 12, pp. 767–776. https://doi.org/10.1166/jon.2023.1923.

[33] Raghunath, K., Mohana Ramana, R., Ramachandra Reddy, V., Obulesu, M., 2023. Diffusion Thermo and Chemical Reaction Effects on Magnetohydrodynamic Jeffrey Nanofluid Over an Inclined Vertical Plate in the Presence of Radiation Absorption and Constant Heat Source. Journal of Nanofluids, 12,pp.147–156. https://doi.org/10.1166/jon.2023.1923.

[34] Raghunath, K., Ali, F., Khalid, M., Abdullaeva, B.S., Altuijri, R., Ijaz Khan, M., 2023. Heat and mass transfer on MHD flow of Jeffrey nanofluid based on Cu and TiO2 over an inclined plate and diffusion-thermo and radiation absorption effects. Pramana (Journal of Physics), 97(4), p.202. https://doi.org/10.1007/s12043-023-02673-3.

[35] Sunitha Rani, Y., Kalyan Kumar, P., Raghunath, K., Asmat, F., 2024. Unsteady MHD rotating mixed convective fow through an infinite vertical plate subject to Joule heating, thermal radiation, Hall current, radiation absorption. Journal of Thermal Analysis and Calorimetry. https://doi.org/10.1007/s10973-024-12954-7.

[36] Hari Babu, K., Raghunath, K., Charankumar, G., Giulio, L., 2023. Heat and Mass Transfer on Unsteady MHD Chemically Reacting Rotating Flow of Jeffrey Fluid Past an Inclined Plates under the Impact of Hall Current, Diffusion Thermo and Radiation Absorption. Journal of Advanced Research in Fluid Mechanics and Thermal Sciences, 111(2), pp. 225–241. https://doi.org/10.37934/arfmts.111.2.225241.

[37] Raghunath, K., Obulesu, M., Sujatha, S., Venkateswararaju, K., 2021. Investigation of MHD Casson fluid flow past a vertical porous plate under the influence of thermal diffusion and chemical reaction. Heat Transfer, 51(9), pp. 377-394. https://doi.org/10.1002/htj.22311.

[38] Raghunath, K., Mohana Ramana R., Veeranna, V., Ijaz Khan, M., Sherzod, A., Nissren, T., 2023. Hall current and thermal radiation effects of 3D rotating hybrid nanofluid reactive flow via stretched plate with internal heat absorption, Results in Physics, Volume 53, 106915. https://doi.org/10.1016/j.rinp.2023.106915.

[39] Raghunath, K., Ramachandra Reddy, V., Ijaz Khan, M., Abdullaev, S.S., Habibullah, A., Boudjemline, Boujelbene, M., Yassine, B., 2023. Unsteady magneto-hydro-dynamics flow of Jeffrey fluid through porous media with thermal radiation, Hall current and Soret effects, Journal of Magnetism and Magnetic Materials, Volume 582, 171033. https://doi.org/10.1016/j.jmmm.2023.171033.

[40] Dash, R.K, Mehta, K.N., Jayaraman, G., 1996. Casson fluid flow in a pipe filled with homogeneous porous medium, International journal of engineering Science, 34, 1145-1156.